Osteoarthritis and Cartilage 27 (2019) 1361–1371

Osteoarthritis and Cartilage

GC–MS method for metabolic profiling of mouse femoral head articular cartilage reveals distinct effects of tissue culture and development

A. Batushansky †, E.B.P. Lopes †, S. Zhu †, K.M. Humphries † ‡ ||, T.M. Griffin † ‡ § || *

† *Aging and Metabolism Research Program, Oklahoma Medical Research Foundation, Oklahoma City, OK, 73104, USA*
‡ *Department of Biochemistry and Molecular Biology, University of Oklahoma Health Sciences Center, Oklahoma City, OK, 73104, USA*
§ *Department of Physiology, University of Oklahoma Health Sciences Center, Oklahoma City, OK, 73104, USA*
|| *Reynolds Oklahoma Center on Aging, University of Oklahoma Health Sciences Center, Oklahoma City, OK, 73104, USA*

ARTICLE INFO

Article history:
Received 16 January 2019
Accepted 14 May 2019

Keywords:
Cartilage
Mouse model
Metabolomics
Serum-free
Femoral head
Development

SUMMARY

Objective: The metabolic profile of cartilage is important to define as it relates to both normal and pathophysiological conditions. Our aim was to develop a precise, high-throughput method for gas/chromatography-mass/spectrometry (GC-MS) semi-targeted metabolic profiling of mouse cartilage.
Method: Femoral head (hip) cartilage was isolated from 5- and 15-week-old male C57BL/6J mice immediately after death for *in vivo* analyses. *In vitro* conditions were evaluated in 5-week-old samples cultured ±10% fetal bovine serum (FBS). We optimized cartilage processing for GC-MS analysis and evaluated group-specific differences by multivariate and parametric statistical analyses.
Results: 55 metabolites were identified in pooled cartilage (4 animals per sample), with 29 metabolites shared between *in vivo* and *in vitro* conditions. Multivariate analysis of these common metabolites demonstrated that culturing explants was the strongest factor altering cartilage metabolism, followed by age and serum starvation. *In vitro* culture altered the relative abundance of specific metabolites; whereas, cartilage development between five and 15-weeks of age reduced the levels of 36 out of 43 metabolites >2-fold, especially in TCA cycle and alanine, aspartate, and glutamate pathways. *In vitro* serum starvation depleted six out of 41 metabolites.
Conclusion: This study describes the first GC-MS method for mouse cartilage metabolite identification and quantification. We observed fundamental differences in femoral head cartilage metabolic profiles between *in vivo* and *in vitro* conditions, suggesting opportunities to optimize *in vitro* conditions for studying cartilage metabolism. In addition, the reductions in TCA cycle and amino acid metabolites during cartilage maturation illustrate the plasticity of chondrocyte metabolism during development.

Introduction

The development of -omics technologies, such as transcriptomics and proteomics, have aided in our understanding of the role of metabolic factors in osteoarthritis (OA) pathophysiology by providing new methodologies to comprehensively examine cartilage biology[1–3]. More recently, metabolomics, which utilizes qualitative and quantitative analyses to evaluate the composition of small molecules (<1.5 kD) in specific tissues or biological fluids[4,5], has also been applied to OA[6–8]. To date, several studies have used metabolomic-based approaches to evaluate metabolite changes in synovial fluid[9–11], synovium[12], serum[13], and urine[14] from healthy and OA patients. These studies have shown distinct metabolic features in OA patients, such as altered levels of the amino acids phenylalanine, tyrosine, proline and glycine among 35 detected metabolites in human synovial fluid[9]. Metabolomic analyses have also been conducted in human OA cartilage, primary chondrocytes, and guinea pig cartilage[15–18]. However, it is not known how cartilage metabolism contributes to OA-related changes in synovial joint metabolites. Conducting cartilage metabolic profiling for systematic studies of OA metabolomics is difficult due to multiple

* Address correspondence and reprint requests to: T. M. Griffin, Aging & Metabolism Research Program, MS 21 Oklahoma Medical Research Foundation, 825 N.E. 13th Street, Oklahoma City, OK, 73104, USA. Tel: 1-405-271-7579
E-mail addresses: albert-batushansky@omrf.org (A. Batushansky), lopese@omrf.org (E.B.P. Lopes), shouan-zhu@omrf.org (S. Zhu), kenneth-humphries@omrf.org (K.M. Humphries), tim-griffin@omrf.org (T.M. Griffin).

https://doi.org/10.1016/j.joca.2019.05.010
1063-4584/

technical challenges associated with being able to collect a sufficient amount of tissue rapidly using either model organisms or human donors.

To address this challenge, our goal was to develop a method for high-throughput metabolic profiling of the mouse articular cartilage. We focused on mouse femoral head cartilage for several reasons. First, the widespread availability of mouse genetic models provides future opportunities to study the role of specific genes in cartilage metabolism. Second, femoral head cartilage can be readily extracted, which is critical for metabolite evaluation. And third, mouse femoral head cartilage explants have been used as an *in vitro* tissue culture model to study genetic and pharmacologic factors involved in cartilage extracellular matrix degradation and inflammation[19,20]. Therefore, we also tested the effect of *in vitro* femoral head explant culture on cartilage metabolites in comparison to metabolites measured in rapidly collected snap-frozen tissue (i.e., "*in vivo*").

Currently, the majority of metabolomics studies are performed using mass spectrometry (MS) coupled with gas or liquid chromatography (GC or LC, respectively). GC-MS provides the most reproducible identification of metabolites by consistent retention time (RT) and mass spectrum under a specific method[21,22]. This consistency makes it possible to identify metabolic compounds using reference libraries for non-targeted tissue metabolic profiling[23]. Therefore, we focused on developing a high-throughput GC-MS-based method by optimizing the entire multi-step process, including the required sample size, tissue collection procedures, metabolite extraction and derivatization, GC-MS separation, compound annotation, and data analysis.

Methods

Animals and experimental design

All experiments were conducted in accordance with protocols approved by the AAALAC-accredited Institutional Animal Care and Use Committee at the Oklahoma Medical Research Foundation (OMRF). C57BL/6J male mice were purchased at four and 14-weeks of age from The Jackson Laboratory (Bar Harbor, ME, USA) and were acclimated within the OMRF vivarium for 1 week prior to conducting experimental procedures. Mice were group housed ($\leq$5 animals/cage) in ventilated cages in a temperature-controlled room maintained at 22 ± 3°C on 14 h:10 h light/dark cycles with *ad libitum* access to chow and water. Animals ($n = 63$) were purchased for three different analyses that focused on 1) sample pooling optimization, 2) *in vitro* cartilage explant analysis, and 3) *in vivo* developmental age comparisons (Fig. 1). Additional animals ($n = 12$) were purchased for histological analyses and to compare the effect of *in vivo* vs *in vitro* conditions on femoral head cartilage proteoglycan staining, aggrecan immunostaining, and aggrecan gene expression as described in the supplemental materials.

Sample collection

Rapid metabolite turnover after animal death prior to sample collection is one of the major contributors to technical variability. To minimize this variability, cartilage from both hips of a single animal were collected into 2mL pre-frozen round bottom plastic tubes with safe lock lids and snap-frozen in liquid nitrogen (LN_2) as quickly as possible after animal death [2.3 ± 0.5 min (mean ± sd)]. We also attempted to minimize variability by collecting samples at a consistent time of day (8am - 9am). Animals were euthanized by rapid cervical dislocation following isoflurane anesthesia. Femoral heads were isolated from 5-week-old mice as previously described[20]. In 15-week-old animals, the epiphysis is fully calcified; therefore, femoral head articular cartilage was harvested using a scalpel blade under a dissection microscope. In both cases, the ligament of the head of the femur was trimmed prior to cartilage collection. Samples were stored at −80°C until further analysis.

For *in vitro* culture experiments, femoral heads were briefly washed in DMEM media with 1% penicillin/streptomycin (PS) before being transferred to a 48-well plate and cultured with DMEM supplemented with 1% PS and 10% fetal bovine serum (FBS). Explants from left and right hips of eight animals were placed in separate paired wells (Fig. 1). Femoral heads were cultured for 48 h at 37°C, 5% CO_2, replacing the media after 24 h. We then tested the effect of 24-h serum starvation by replacing the media with DMEM 1% PS media supplemented with or without 10% FBS in wells with animal-matched explant pairs. After 24 h, the samples were briefly washed in one mL saline solution (37°C), transferred to two mL tubes, frozen in LN_2, and stored at −80°C until further analysis.

Metabolite extraction

A classic methanol:chloroform:water extraction procedure[24] was used as a basis for this method with substantial modifications for cartilage. Pooled tissue was homogenized under LN_2 using a Qiagen TissueLyser II. Immediately following, 500 μL of methanol was added to each sample and vigorously vortexed. Next, 10 μL of internal standard (ISTD, ribitol, 20 mg/mL in water) was added. The samples were vortexed, sonicated for 2 min, and placed on an orbital shaker at 70°C. After 10 min of incubation, 250 μL of pure chloroform was added to each sample, vortexed for 10 s, mixed with 250 μL of water, and vortexed. The samples were then centrifugated for 15 min at 14,000 rpm.

Next, 500 μL of supernatant was transferred to a new two mL tube for a two-stage evaporation and concentration step. 300 μL supernatant was transferred to a 400 μL glass insert placed into a new two mL tube, which was placed in an Eppendorf Vacufuge for 1 h. The use of 400 μL inserts provided an effective compromise between sufficient surface area for efficient evaporation and a small diameter that allowed a smaller volume of derivatization agents. Reduced volume created a more concentrated sample, which was beneficial for testing small amounts of cartilage tissue. In parallel, the second fraction of supernatant was stored at +4°C to avoid metabolite degradation. After an hour, the Vacufuge was stopped to add the second supernatant fraction to the insert tube, and drying was completed in the Vacufuge for another 3 h.

In parallel with the sample processing, individual external standards of pyruvate, lactate, 3-hydroxybutyrate, leucine, glucose, fructose and fructose-6-phosphate were prepared and dried alongside with the samples. This step served two purposes - selective confirmation of library-based metabolite annotation and quality control analysis (QC). Considering the limited amount of tissue, we did not apply an often-used procedure for QC that consists of pooled sub-fractions of all samples subjected for the GC-MS analysis. Instead, external standards were used as QCs. Fully dried samples were then derivatized.

Derivatization

Derivatization chemically modifies compounds to improve their detectability by GC-MS. We adjusted a standard trimethylsilyl (TMS)-based derivatization procedure[24] for cartilage. Briefly, dried samples were dissolved in 25 μL of methoxyamine hydrochloride in pyridine (20 mg/mL) for 90 min at 37°C under the constant orbital shaking (1,100 rpm). Next, 40 μL of N,O-Bis(trimethylsilyl)trifluoroacetamide (BSTFA) were added to each sample and shaken at 37°C for an additional 30 min. Lastly, 10 μL of C_{10}–C_{40} alkanes mixture were added to each sample to serve as

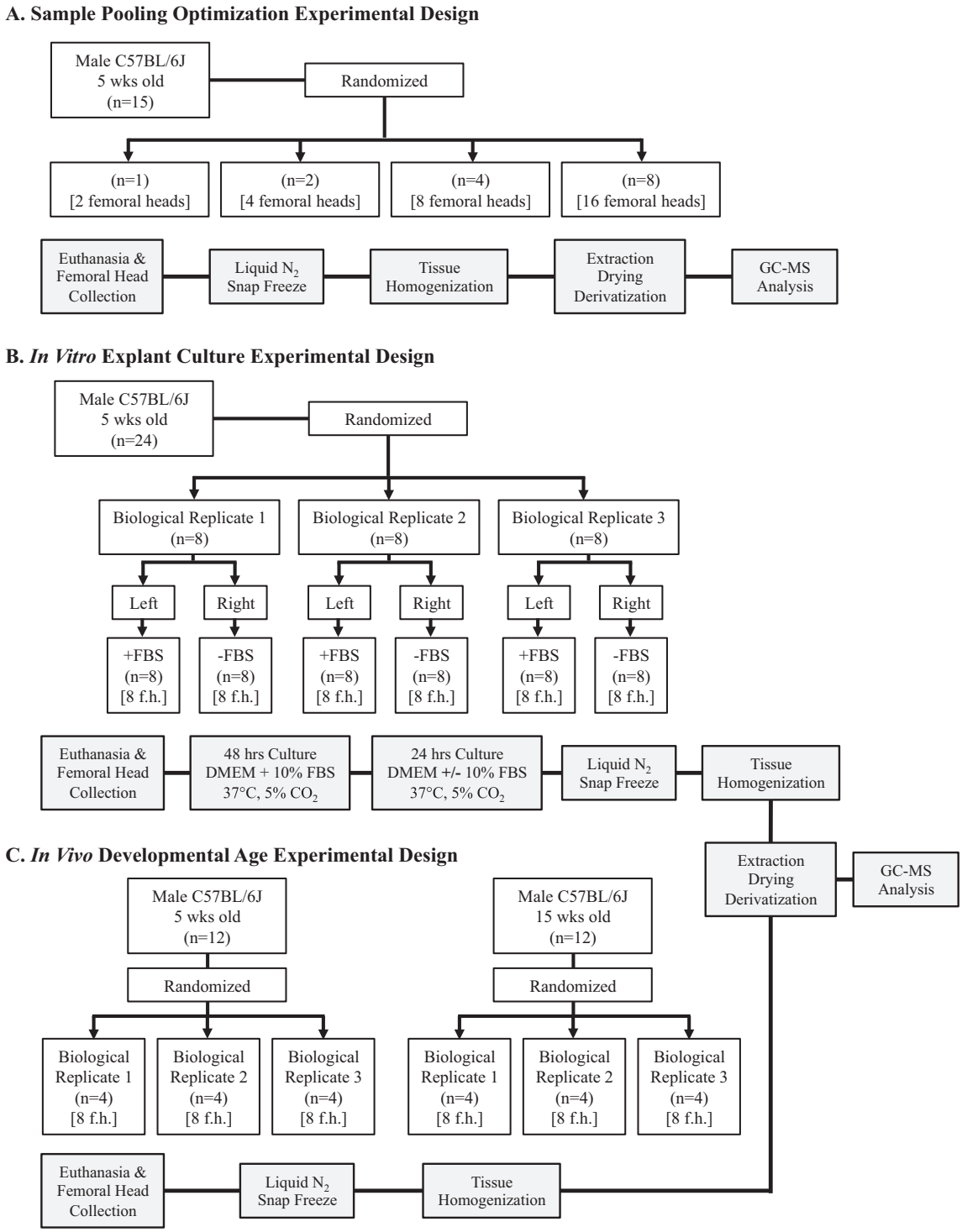

Fig. 1. Overview of experimental design (open boxes) and sample workflow (filled boxes). A. We compared the number of metabolites that could be detected in samples composed of femoral head cartilage pooled from the left and right limbs of 1, 2, 4, and eight mice per sample. The optimal sample size pooling balanced maximizing the number of detected metabolites with animal usage. B. *in vitro* explant culture experiments were conducted to compare fetal bovine serum (FBS) "fed" vs "starved" conditions and to compare to *in vivo* conditions. Femoral head pairs were isolated from an individual animal and separated into either a +FBS or −FBS group so that comparisons were biologically matched. Based on results from the optimization experiment, we pooled eight femoral heads (f.h.) for each biological sample. C. *in vivo* experiments compared femoral head cartilage extracted immediately following death from 5-week and 15-week-old animals. Each experimental *in vivo* or *in vitro* group consisted of three independent biological replicates, with each replicate composed of eight femoral heads pooled from 4 to 8 animals as indicated. To minimize potential technical variation for *in vitro* and *in vivo* comparisons, stored frozen samples were simultaneously homogenized, processed for metabolite extraction and derivatization, and analyzed by GC-MS. Group differences were initially evaluated by principle component analysis followed by statistical testing.

time standards, and the samples were shaken for another 10 min. In parallel, one blank sample (only derivatization reagents) and one blank-alkane sample were prepared under the same conditions. Next, the inserts with samples were transferred into the GC-MS vials, immediately closed with vial screw-caps, and placed into the automatic liquid sampler (ALS) of the GC-MS system. We randomized the order of samples within *in vivo* and *in vitro* conditions to minimize a potential effect of cross-contamination on the results.

GC–MS run parameters

We used an Agilent 7890B-5977A GC-MS system equipped with 7650 ALS, HT-5 MS 30 m capillary column and EI source for the metabolite analysis. 1 μL of sample was automatically injected in splitless mode and analyzed under the following conditions: initial oven temperature was set to 70°C and held for 1 min, then ramped to 120°C by 5°C/min, then to 280°C by 12°C/min, and then to 300°C by 20°C/min and held for 1 min. A full scan from 60 to 600 *m/z* was performed. The single run time was ~26 min.

Metabolite annotation

The obtained chromatograms were processed using Agilent MassHunter Quantitative Data Analysis software with integrated mass-spectrometry library from the National Institute of Standards and Technology (NIST, Gaithersburg, USA). The metabolites were annotated according to the selected analytical standards and NIST library. The relative abundance of metabolites was calculated by peak area and normalized according to the sample wet weight and internal standard.

Data analysis

Based on our preliminary sample size determination experiment (Fig. 2), cartilage was pooled from left and right hips of four animals for a single biological replicate. Thus, twelve animals per experimental group were used to form three biological replicates ($n = 3$) (Fig. 1). Each extracted sample was injected into the GC-MS twice to control for technical repeatability of the analysis. For the statistical tests, mean values of the technical duplicates were used ($n = 3$), except for principal component analysis (PCA), which was performed using biological and technical replicate samples ($n = 6$/group). Principal components analysis (PCA), Dunnett's test, Student's *t*-test, ternary plots, and heat-maps were performed using *SimComp*-, *stats*-, *plotly*- and *ggplot2*-packages for R-project (v.3-5-2)[25–27]. Multivariate and univariate statistical analyses were performed on $\log_{10}$-transformed data. Venn diagrams were built using the online available tool Venny 2.0 (http://bioinfogp.cnb.csic.es/tools/venny). Pathway analysis was performed using MetaboAnalyst web-platform[28] on KEGG database background[29].

Results

Pooled sample size determination

Due to the small size of mouse femoral head cartilage, we first sought to optimize animal usage and metabolite detection by comparing metabolic profiles of four samples that consisted of left and right femoral heads collected and pooled from $n = 1$, $n = 2$, $n = 4$, and $n = 8$ 5-week old animals. The average weight of each femoral head pair was 5.1 mg, and the estimated range was 4.2–6.2 mg [Fig. 2(A)]. The strong correlation between total sample weight and number of animals per pooled samples demonstrated

A

Parameter	Sample 1	Sample 2	Sample 3	Sample 4	Mean	StDev
# of pooled animals	1	2	4	8		
Weight of the sample, mg	5.1	12.4	18.9	33.9		
Weight of a single femoral head pair, mg	5.1	6.2	4.725	4.2375	5.066	0.72

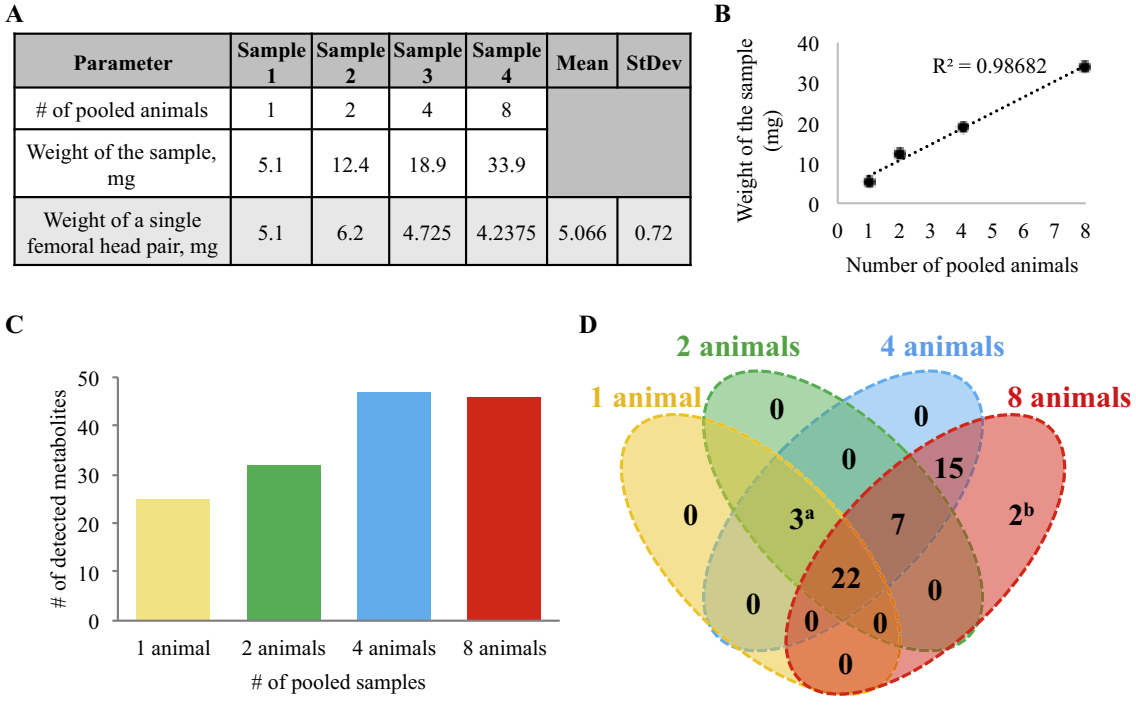

Fig. 2. Sample size pooling determination. Given the small amount of tissue obtained from the proximal femoral head cartilage of mice, we performed preliminary tests to determine the number of metabolites that could be detected in left-right femoral head pairs pooled from 1, 2, 4, and 8 animals. A. Total weight of the collected cartilage per pooled sample and the calculated paired femoral head mass per animal. B. Total sample weight vs pooled sample number showed a strong linear correlation. C. The number of metabolites detected in each pooled sample increased from one to four pooled samples but did not increase further with eight pooled samples. D. Venn diagram of overlapped metabolites detected between the different pooled sample sizes. [a]Metabolites not detected in samples pooled from eight animals due to signal over-saturation (lactate, glucose, and myo-inositol). [b]Metabolites only detected in samples pooled from eight animals due to low abundance (3-hydroxybutyrate, sorbitol).

consistent sample sizes and harvesting proficiency [Fig. 2(B)]. Samples were then qualitatively compared to determine the number of detectable metabolites for each pooled sample size [Fig. 2(C)]. 25 metabolites were detected in cartilage from one animal. This increased to 32 metabolites detected from two animals and 47 metabolites from four animals. However, only 46 metabolites were detected in cartilage pooled from eight animals. Two additional low-abundance metabolites were identified in this largest sample (hydroxybutyrate and sorbitol), but three metabolites were not quantifiable due to saturated peak intensities (lactate, glucose and myo-inositol) [Fig. 2(D)]. Therefore, we decided to pool cartilage from four animals as a single biological replicate to optimize metabolite detection in the fewest number of animals.

Overall comparison of GC–MS metabolic profiles between cartilage conditions

Following the optimization of sample size pooling, we designed an experiment that included four experimental groups with each one consisting of three biological replicates composed of eight femoral heads pooled from four or eight animals (Fig. 1). Thus, the tissue wet-weights were similar among all comparisons. Results were normalized by an internal standard (ribitol) and total sample wet weight. The experimental groups were designed to evaluate the qualitative and quantitative variation in cartilage metabolites across three conditions. First, we compared 5-week old cartilage metabolites between *in vivo* and *in vitro* conditions to explore the potential translation of the results obtained from *in vitro* culture conditions to the *in vivo* setting. Second, we tested the effect of postnatal development from five- to 15-weeks on i*n vivo* cartilage metabolites to evaluate metabolic plasticity of chondrocytes between the phase of cartilage mineralization and mature articular cartilage. Third, we evaluated the effect of 24-hrs of FBS starvation on *in vitro* cartilage metabolites to determine the magnitude of this common pre-treatment condition on overall metabolite changes and how they compare to the *in vivo* setting.

Combining all the experimental groups together, 55 (Supplemental data 1 and 2) unique compounds belonging to sugars, sugar alcohols, carboxylic acids, amino acids, N-enriched compounds, and fatty acids were identified (Table I). When comparing *in vivo* and *in vitro* samples, only 29 metabolites were identified in both groups (Table I). However, 43 metabolites were identified in 5-week and 15-week old *in vivo* cartilage samples. Similarly, 41 metabolites were identified in FBS-treated vs FBS-starved *in vitro* samples. Thus, the greatest qualitative differences in cartilage metabolic profiles occurred comparing *in vivo* and *in vitro* conditions.

Comparison of GC–MS metabolic profiles between in vivo and in vitro cartilage samples

To further explore the *in vivo* vs *in vitro* differences, we found that 14 metabolites were exclusive to *in vivo* samples, and 12 metabolites were exclusive to *in vitro* samples [Fig. 3(A)]. Substantial differences between *in vivo* and *in vitro* conditions were still observed by PCA when evaluating the 29 metabolites that were detected in both groups [Fig. 3(B)]. PC_1, which explained 68% of data variance, was primarily determined by variance between *in vivo* and *in vitro* sample groups [Fig. 3(B)]. These metabolite differences were not associated with appreciable changes in Safranin-O staining for glucosaminoglycans [Fig. 3(C)], aggrecan immunostaining [Fig. 3(D)], or aggrecan gene expression ($p = 0.24$) [Fig. 3(E)]. The second largest source of variation was PC_2, which explained 25% of data variance. This showed a clear effect of cartilage developmental stage within *in vivo* samples, while the effect of FBS was the weakest among the experimental conditions [Fig. 3(B)].

We examined the differences in metabolite levels between *in vivo* and *in vitro* 5-week old cartilage samples by generating ternary plots that included the *in vivo* sample and the FBS+ and FBS- *in vitro* samples [Fig. 4(A)]. Ternary plots are graphical diagrams that allow the relative level of an output to be compared among three conditions. Thus, for our purposes, the ternary plot shows the relative content of each identified metabolite in respect to its total abundance among all three groups. Both FBS+ and FBS- *in vitro* samples were included to determine if one condition was more similar to *in vivo* values. To simplify the comparisons, metabolites were separated with respect to their prevalence in nitrogen-based and carbon-based metabolic pathways [Fig. 4(A)]. Ten nitrogen-based metabolites (40%) were enriched in the *in vivo* cartilage samples (i.e., aspartate, pipecolic acid, sarcosine, creatinine, hydroxyproline, alanine, glutamate, serine, methionine and oxoproline; Fig. 4(A),(C)). A slightly smaller number of metabolites were intermediate among all conditions (i.e., proline, glycine, valine, threonine, leucine, phenylalanine and taurine), and several metabolites were enriched in cartilage cultured *in vitro* with FBS (i.e., asparagine, glutamine, isoleucine, tyrosine, β-alanine, citrulline, and urea). These metabolites were enriched in the FBS-treated medium belong to the main nitrogen-related pathways of amino acid and urea metabolism. Only one nitrogen-based metabolite was enriched in the cartilage cultured *in vitro* without FBS (aminomalonic acid).

In contrast to nitrogen-based metabolites, carbon-based metabolites were overwhelmingly enriched in *in vivo* cartilage samples (73%; Fig. 4(B) and (C)). Several of these metabolites were only detected in cartilage harvested under *in vivo* conditions, including glucose, allose, mannose, lactose, maltose, scyllo-inositol, 3-hydroxybutyrate, glycerate, threonate, fumarate, oxoglutarate [Fig. 4(C)]. Given the uncertainty in the identification of some sugars via library match (Table I), the non-glycolytic or TCA cycle sugars from this list may represent a generally greater content of mono- and di-saccharides and their phosphorylated forms in the freshly collected cartilage tissue compared to *in vitro* groups. A small number of carbon-based metabolites were enriched among *in vitro* samples, with slightly more in FBS-treated (i.e., sorbose, sorbitol, glycerol) compared to FBS-starved conditions (i.e., oleic and phosphoric acids) [Fig. 4(B) and (C)].

Effect of cartilage maturation on GC–MS metabolic profile

Although the femur as a whole undergoes substantial developmental changes between five- and 15-weeks of age, femoral head size is consistent [Fig. 5(A)]. Many chondrocytes in 5-week-old femoral heads are hypertrophic; whereas, by 15-weeks of age, the physis and epiphysis have ossified leaving a thin surface of articular cartilage [Fig. 5(B)]. Despite these differences, the weights of cartilage samples from five to 15-week-old animals, which were used for normalization of the metabolite abundance, were similar [Fig. 5(C)]. Per unit area, though, the cellular density was 1.45 times greater in 15 vs 5-week-old cartilage (3.5×10^3 vs 2.4×10^3 cells per mm^2, respectively).

We observed a broad reduction in metabolite levels in cartilage from 15- vs 5-wk-old animals. Of the 43 detected metabolites, 38 were significantly depleted as determined by Student's *t*-test with FDR-correction for multiple testing (Fig. 5(D); Supplemental Data 3(A)). The TCA cycle intermediates citrate, succinate, fumarate and malate, as well as the branched-chain amino acids valine and leucine, were depleted more than 2-fold. Other amino acids demonstrated even stronger decline. For example, proline and

Table I
Annotation of detected metabolites by NIST library and external standards. For library-matched metabolites, the average retention time (RT), Kovats retention index (RI), and match probability are provided. For the metabolites confirmed by external standards, probability match is unnecessary. Experimental route column indicates the experimental condition(s) in which the metabolite was detected

Name	Average RT, min	RI	Library RI	ΔRI	Library match, %	Experimental route
Decane	5.83	1,000	n/a (control)	n/a	n/a	*in vivo*, *in vitro*
Pyruvate	6.81	1,046	1,056	10	external standard confirmed	*in vivo*, *in vitro*
Lactate	7.07	1,058	1,066	8	external standard confirmed	*in vivo*, *in vitro*
Alanine	7.97	1,100	1,095	−5	77	*in vivo*, *in vitro*
Glycine	8.36	1,118	1,105	−13	89	*in vivo*, *in vitro*
Oxalic acid	8.91	1,143	1,136	−7	16	*in vivo*, *in vitro*
3-hydroxybutyrate	9.13	1,153	1,167	14	68	*in vivo*
beta-Alanine	10.04	1,196	1,190	−6	45	*in vitro*
Dodecane	10.13	1,200	n/a (control)	n/a	n/a	*in vivo*, *in vitro*
Valine	10.74	1,228	1,224	−4	77	*in vivo*, *in vitro*
Urea	11.17	1,252	1,279	27	98	*in vitro*
Leucine	12.07	1,297	1,289	−8	external standard confirmed	*in vivo*, *in vitro*
Glycerol	12.20	1,303	1,290	−13	43	*in vitro*
Isoleucine	12.50	1,319	1,299	−20	external standard confirmed	*in vitro*
Proline	12.51	1,319	1,305	−14	94	*in vivo*, *in vitro*
Succinate	12.82	1,335	1,321	−14	70	*in vivo*, *in vitro*
Glycerate	13.25	1,356	1,344	−12	16	*in vivo*
Fumarate	13.39	1,363	1,353	−10	71	*in vivo*
Nonanoic acid	13.55	1,371	1,355	−16	85	*in vivo*
Pipecolic acid	13.69	1,378	1,363	−15	22	*in vivo*
Serine	13.74	1,381	1,368	−13	83	*in vivo*, *in vitro*
Sarcosine	13.93	1,390	1,568	178	14	*in vivo*
Tetradecane	14.12	1,400	n/a (control)	n/a	n/a	*in vivo*, *in vitro*
Threonine	14.17	1,404	1,401	−3	96	*in vivo*, *in vitro*
Aminomalonic acid	15.30	1,493	1,485	−8	78	*in vivo*, *in vitro*
Malate	15.68	1,522	1,507	−15	88	*in vivo*, *in vitro*
Methionine	15.87	1,538	1,531	−7	83	*in vivo*, *in vitro*
Oxoproline	15.87	1,538	1,522	−16	84	*in vivo*, *in vitro*
Aspartate	15.93	1,542	1,544	2	73	*in vivo*
Hydroxyproline	16.00	1,547	1,504	−43	81	*in vivo*, *in vitro*
Creatinine	16.34	1,574	1,559	−15	47	*in vivo*, *in vitro*
Threonic acid	16.49	1,586	1,523	−63	60	*in vivo*
Glutamine	16.49	1,586	1,545	−41	17	*in vivo*, *in vitro*
Hexadecane	16.67	1,600	n/a (control)	n/a	n/a	*in vivo*, *in vitro*
Citrulline	16.81	1,614	unknown	unknown	17	*in vitro*
Glutamate	17.05	1,638	1,651	13	95	*in vivo*, *in vitro*
Phenylalanine	17.10	1,643	1,636	−7	70	*in vivo*, *in vitro*
Taurine	17.59	1,692	1,600	−92	98	*in vivo*, *in vitro*
Xylitol	18.12	1,745	1,738	−7	18	*in vivo*, *in vitro*
Ribitol	18.25	1,758	1,746	−12	58	*in vivo*, *in vitro*
Phosphoric acid	18.55	1,788	1,780	−8	94	*in vitro*
Octadecane	18.67	1,800	n/a (control)	n/a	n/a	*in vivo*, *in vitro*
Citrate	19.06	1,835	1,845	10	94	*in vivo*, *in vitro*
Asparagine	19.20	1,847	unknown	unknown	8	*in vitro*
Tyrosine	19.57	1,881	unknown	unknown	21	*in vitro*
Fructose	19.66	1,889	1,859	−30	external standard confirmed	*in vivo*, *in vitro*
Sorbose	19.71	1,893	1,863	−30	15	*in vitro*
Glucose	19.86	1,907	1,901	−6	external standard confirmed	*in vivo*, *in vitro*
Sorbitol	20.19	1,937	1,920	−17	19	*in vitro*
Lactose	20.30	1,947	1,939	−8	10	*in vivo*
Allofuranose	20.40	1,956	1,852	−104	21	*in vivo*, *in vitro*
Maltose	20.48	1,963	1,975	12	16	*in vivo*
Palmitic acid	20.79	1,991	2,050	59	98	*in vivo*, *in vitro*
Ribose	21.16	2,024	unknown	unknown	6	*in vivo*, *in vitro*
Scyllo-inositol	21.40	2,046	unknown	unknown	77	*in vivo*, *in vitro*
Myo-inositol	21.44	2,049	2,113	64	87	*in vivo*, *in vitro*
Docosane	21.95	2,200	n/a (control)	n/a	n/a	*in vivo*, *in vitro*
Oleic acid	22.11	2,223	2,218	−5	19	*in vitro*
Stearic acid	22.29	2,248	2,246	−2	98	*in vivo*, *in vitro*
Allose	23.11	2,363	2,316	−47	15	*in vivo*
Mannose	23.19	2,375	2,324	−51	21	*in vivo*
Tetracosane	23.37	2,400	n/a (control)	n/a	n/a	*in vivo*, *in vitro*

glutamate were reduced 8–9-fold, glycine was reduced 6-fold, and serine, aspartate, alanine, threonine and methionine were reduced 3–5-fold (Fig. 5(D), Supplemental Data 3(A)). Only five out of 43 metabolites (i.e., fructose, glycerate, nonanoic, palmitic and stearic acids) did not significantly change between five- and 15-week-old cartilage samples. Considering these broad alterations, we performed a pathway analysis to test if the altered metabolites were linked to specific metabolic pathways. The results indicated that the TCA cycle, galactose metabolism, and several amino acid metabolic pathways (i.e., branched-chain amino acids, glycine-serine-threonine, and alanine-aspartate-glutamate metabolism) were significantly down-regulated in 15-week old samples

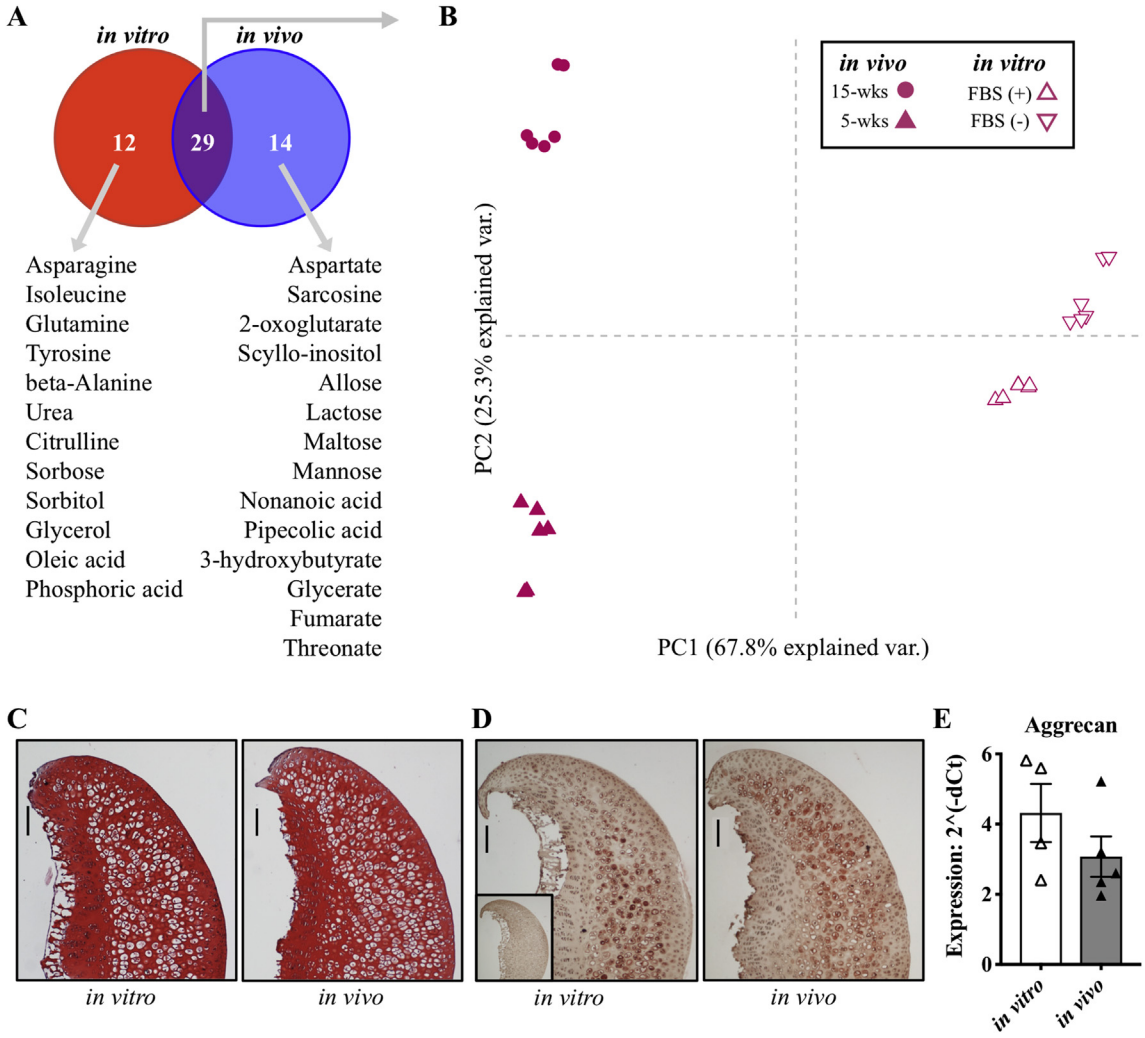

Fig. 3. Comparative analysis of cartilage metabolic profiles. All sample conditions were compared based on metabolite detectability and principal components analysis (PCA) to evaluate variability. A. Venn diagram of metabolites detected in *in vivo* and *in vitro* samples. Metabolites that were uniquely detected in either set of samples are listed below their respective circle. Additional details are provided in Table I and Supplemental data one and 2. B. principal component analysis (PCA) results based on metabolite abundance values for metabolites common to both *in vitro* and *in vivo* samples. The variance explained by each component is indicated on the axes. Note that the *in vitro* samples were obtained from 5-week-old animals, indicating substantial variance in metabolite levels between *in vitro* and *in vivo* conditions. C. *in vitro* (+FBS) and *in vivo* femoral head sections stained with Safranin-O, fast green, and hematoxylin. Bars = 100 μm. D. Aggrecan immunohistochemistry for *in vitro* (+FBS) and *in vivo* femoral head sections (inset: negative control). E. Quantitative gene expression results for aggrecan (*Acan*) based on RNA isolated from *in vitro* (+FBS) and *in vivo* femoral head cartilage.

(q_{FDR}<0.05; Fig. 5(E)). Thus, these changes suggest that substantial reductions in free metabolites involved in biosynthetic pathways occur between five- and 15-weeks.

Discussion

The aim of this work was to develop a method for high-throughput profiling of the mouse articular cartilage metabolites. Metabolic stress, especially in the context of obesity and metabolic syndrome, is a critical factor and perhaps even a distinct pathway leading to the development of OA[2,30]. It is not clear, however, to what extent this association is due to direct metabolic effects on joint tissues vs activation of metabolic inflammatory pathways[31]. This optimized method for conducting mouse articular cartilage metabolic profiling using GC-MS illustrates the sensitivity of cartilage metabolite detection through three different comparisons: 1) *in vivo* vs *in vitro* conditions, 2) effect of 24-hrs of FBS starvation under *in vitro* conditions, and 3) effect of postnatal development from five- to 15-weeks of age under *in vivo* conditions.

In vitro cartilage metabolism research has a 90-year history[32–34]. More recent studies show the dominance of glycolysis for chondrocyte ATP supply[2,35], how metabolic substrate availability is coupled to utilization[36,37], and the positive relationship between oxygen tension and glycolysis[38,39]. However, translating *in vitro* findings to *in vivo* conditions is critical for understanding how chondrocyte metabolic sensing regulates cellular homeostasis and OA risk[2,31,40].

We found substantial differences in cartilage metabolites between *in vivo* and *in vitro* conditions. Metabolites from *in vivo* samples were strongly enriched in sugars and carboxylic acids compared to *in vitro* samples. Conversely, *in vitro* samples were enriched with more nitrogen-based compounds. Amino acids are actively transported in cultured chondrocytes[41] and are critical mediators of mechanistic target of rapamycin complex 1 (mTORC1) pathway activation[42,43]. In particular, we observed increased levels of glutamine and the branched chain amino acid isoleucine from *in*

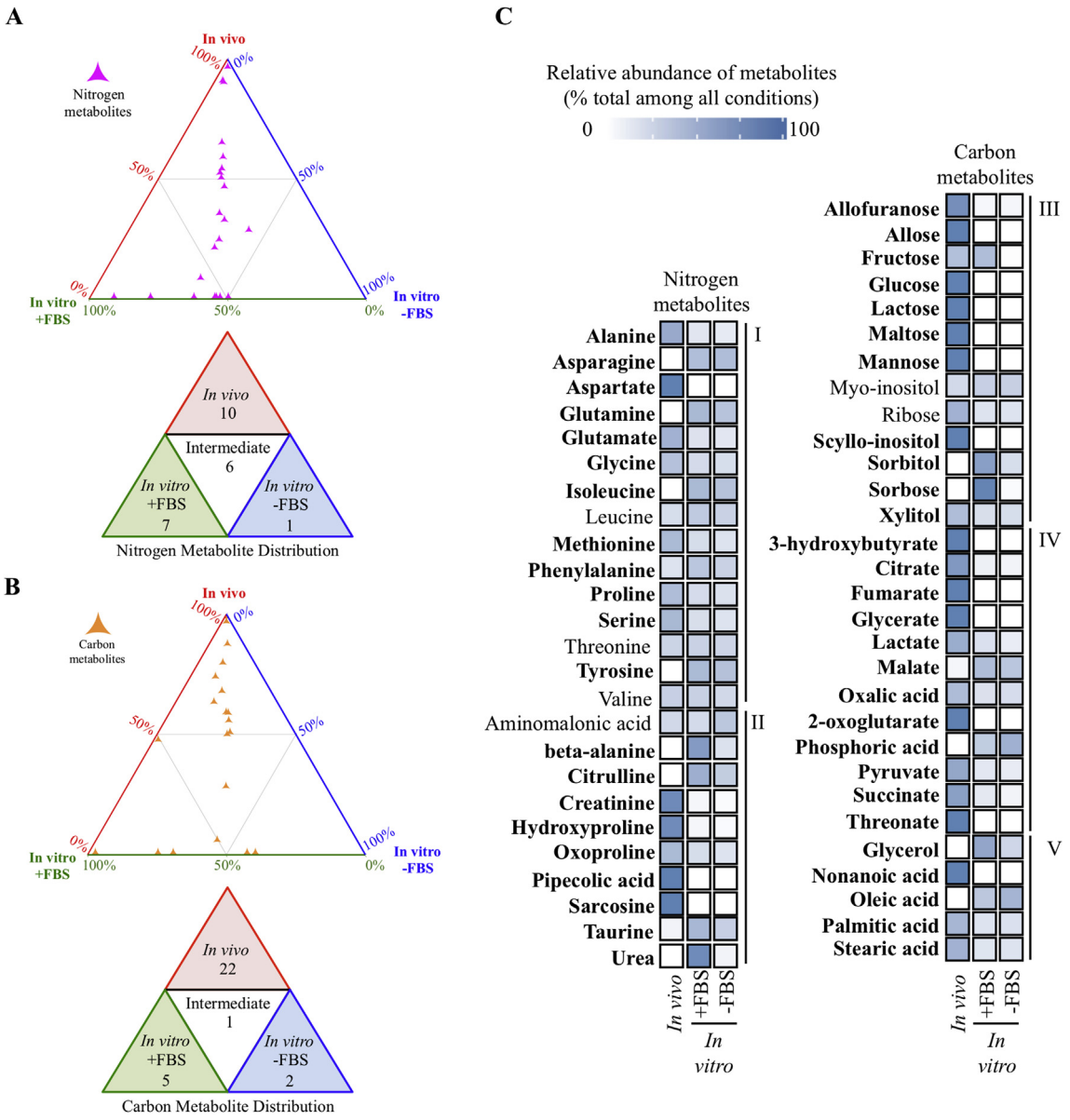

Fig. 4. Relative content of metabolites detected in cartilage collected under *in vivo* or *in vitro* conditions from 5-week-old animals. A. Ternary plot and enrichment distribution summary of nitrogen-based metabolites among *in vivo*, *in vitro* +FBS, and *in vitro* −FBS experimental conditions. B. Ternary plot and enrichment distribution summary of carbon-based metabolites among *in vivo*, *in vitro* +FBS, and *in vitro* −FBS experimental conditions. C. Detailed heat-map of metabolite content, expressed as a percent of the total content among all three experimental conditions. Metabolites are alphabetically ordered within five groups accordingly to their compound class (I: proteinogenic amino acids, II: nitrogen-rich compounds, III: sugars, IV: carboxylic and inorganic acids, V: glycerol and fatty acids). Bold font represents metabolites that changed significantly in *in vivo* compared to *in vitro* +FBS and/or *in vitro* −FBS according to Dunnett's test (Log-transformed raw data, $n = 3$ per group, $P < 0.05$, Supplemental data 4). Note that metabolites only detected under *in vivo* or *in vitro* conditions, as specified in Fig. 3(A), are included in this list.

vitro cultured samples. Conversely, we observed lower levels of glucose, pyruvate, citrate, and succinate in the free metabolite pool of cultured femoral heads, consistent with increased mTORC1 activation[44]. Hypoxia inhibits mTORC1 signaling[45]; however, femoral head explants were cultured under atmospheric oxygen (~21%). Given that cartilage oxygen tension is estimated to be ~2–5% *in vivo*[46], an increase in oxygen tension and greater bioavailability of metabolic signaling factors, such as amino acids, may underlie *in vitro* vs *in vivo* metabolite differences. Future optimization of culture conditions are needed for *in vitro* studies, especially considering how metabolism interfaces with cellular processes involved in OA pathophysiology, such as mTORC1 signaling[47].

A common practice for *in vitro* studies is to remove FBS from culture media 24 h prior to initiating a treatment, often referred to as "serum starvation." Typical FBS preparations contain undefined quantities of growth factors, hormones, and other metabolites, which may interfere with treatment effects and confound the interpretation of results. An additional potential effect of serum starvation is to alter cellular metabolism or better model *in vivo* conditions. Here we detected only minor changes in metabolite content in cartilage explants following 24 h of serum starvation. Specifically, six compounds were significantly reduced (Supplemental file 3(B)). Interestingly, three compounds – fructose, sorbose and sorbitol – are sugars that indirectly enter glycolysis, and another three – urea, creatinine and hydroxyproline

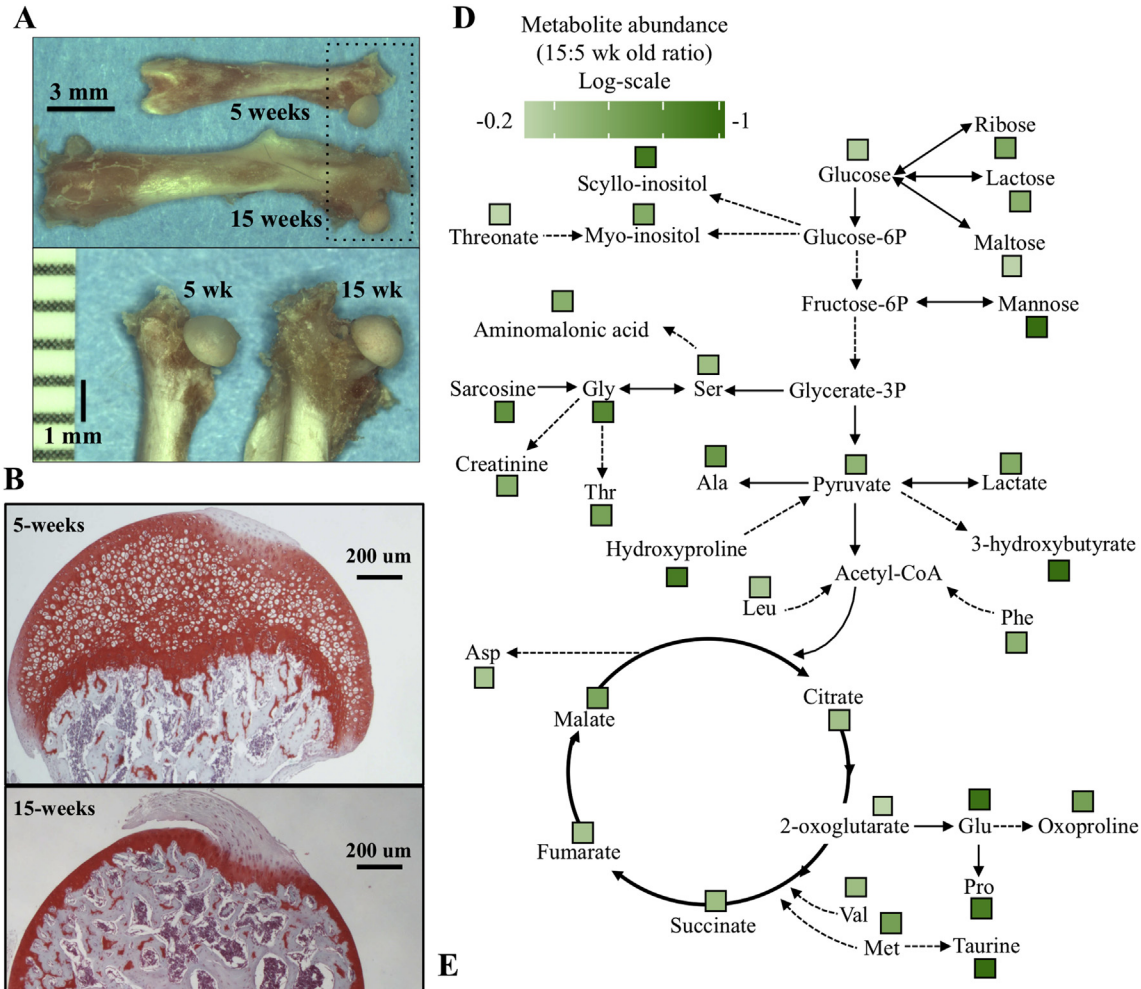

C

Name	Age, weeks	Weight, mg	Mean	StDev
S1	5	15.5	16.81	0.94
S2	5	17.7		
S3	5	17.2		
S4	15	11.7	15.27	3.12
S5	15	19.3		
S6	15	14.8		

E

Pathway	Total	Expected	Hits	Raw p	FDR	Impact
Alanine, aspartate and glutamate	24	0.56	7	5.00 E-07	2.05 E-05	0.52
TCA cycle	20	0.47	6	3.06 E-06	8.36 E-05	0.29
Glycine, serine and threonine	31	0.72	5	5.50 E-04	9.07 E-03	0.57
Valine, leucine and isoleucine	11	0.26	3	1.67 E-03	2.29 E-02	0.67
Galactose	26	0.64	4	3.17 E-03	3.72 E-02	0.05
Arginine and proline	44	1.02	5	2.84 E-03	3.33 E-02	0.20

Fig. 5. Changes in cartilage metabolites during hip development. A. Gross morphological comparison of femur (top panel) and proximal femur (dashed box top panel; bottom panel) between five- and 15-week old mice. Note the similarity in femoral head size despite shorter femur length in 5-week old sample. B. Prior to epiphyseal ossification, mouse femoral heads can be readily isolated and cultured for conducting explant studies. At 5-weeks of age, the epiphyseal cartilage is mineralized and avascular. By 15-weeks, the physis is resorbed and the epiphysis is ossified, leaving a thin layer of articular cartilage. Cartilage was rapidly extracted by gross dissection with a scalpel while minimizing inclusion of subchondral bone and the ligament of the head of the femur. C. Sample wet weights. Metabolite data were normalized to wet weight and internal standards. D. Map (based on KEGG database) of significantly declined metabolites in 15- vs 5-wk old samples based on Student's *t*-test, q_{FDR}<0.05. All metabolites were reduced with increasing age. E. Analysis of significantly down-regulated pathways in 15-week old samples compared to 5-week old samples using MetaboAnalyst web-platform[28] on KEGG database background[29].

– are nitrogen-enriched non-proteinogenic compounds. Further work is required to understand the significance of these changes, although the current findings do not suggest that major alterations occur or that serum starvation models *in vivo* conditions better or worse than standard culture conditions.

We tested the sensitivity of our method to differentiate chondrocyte metabolic phenotypes by comparing five- vs 15-week old femoral head cartilage. The mouse hip epiphysis undergoes a prolonged period of cartilage calcification from 4 to 12 weeks prior to resorption of the physis and replacement with trabecular bone by 15 weeks of age[48]. Thus, at 5-weeks of age, femoral head cartilage is avascular, calcified, and primarily composed of hypertrophic chondrocytes (Fig. 5(A);[48]). The metabolism of hypertrophic chondrocytes, as elucidated from growth plate cartilage, is

characterized by greater mitochondrial content and reliance on oxidative phosphorylation compared to resting-zone growth plate chondrocytes and articular chondrocytes[49,50]. This increase in mitochondrial content and activity in hypertrophic chondrocytes may be related to enhanced calcium handling for matrix calcification. In our comparison, there was a broad reduction in metabolite concentrations in 15-week old articular cartilage compared to 5-week-old calcified cartilage composed largely of hypertrophic chondrocytes. The metabolic pathways that were primarily downregulated involved amino acid metabolism and the TCA cycle, consistent with less mitochondrial metabolism in articular cartilage chondrocytes compared to hypertrophic growth chondrocytes. Future studies are needed to determine if the methodology established here can be applied to detect potentially more subtle differences in chondrocyte metabolism that occur with aging, obesity, or injury in articular cartilage.

There are several limitations to our study. First, our results are mostly based on the metabolic profile of calcified epiphyseal femoral head cartilage harvested from young animals. Although we show that the method can be applied to hip articular cartilage, additional studies are needed to test other joints (e.g., knee) and conditions (e.g., age, diet, exercise). Another potential limitation is the proper selection of a normalization strategy. In this study samples were normalized by wet-weight; however, cartilage contains heterogeneous populations of cells. Tissue-based homogenization methods may mask cell-type specific responses. Future work may benefit from bioinformatic-based normalization and data integration approaches[51]. Furthermore, the identification of additional metabolites with alternate instrumentation (i.e., LC-MS/MS) could provide greater coverage of metabolic pathways and improve bioinformatic analyses. Finally, our treatment comparisons were based on three independent biological replicates (each composed of samples from 4 to 8 animals), which may be insufficient to detect smaller differences and should be further evaluated to assess reproducibility.

In summary, we report the first method for GC-MS metabolic profiling of mouse femoral head cartilage for investigating cartilage metabolic alterations under different conditions, including *in vivo* and *in vitro* studies. Cellular metabolism is intricately linked to anabolic and catabolic processes, homeostasis, and signaling. Consequently, metabolic profiling can help to define tissue development, repair, and response to stress factors[52]. Metabolomics of joint tissues is a promising tool for better understanding the etiology of joint pathologies[53,54], and we believe that development of a method for cartilage tissue GC-MS metabolic profiling can be widely applicable to future studies.

Contribution

AB and TG developed the concept and designed the experiments. AB, EBPL and SZ performed experiments. AB, EBPL and TG analyzed and interpreted the data. AB, EBPL, KH and TG drafted the article. All authors read and approved the final version of the article.

Competing interest statement

There are no conflicts of interest.

Role of the funding source

Supported by the NIH (R01AG049058, 5P30GM114731) and an equipment grant from the Oklahoma Center for Adult Stem Cell Research (OCASCR), a program of TSET. The content is solely the responsibility of the authors and does not necessarily represent the official views of the National Institutes of Health or OCASCR.

Acknowledgements

We thank Dominic Cortassa, Dr. Richard dela Cruz, Pavithra Premkumar, and the OMRF Imaging Core for technical assistance. We also thank Drs. Mary Beth Humphrey and Matlock Jeffries for their helpful suggestions during the development of the study and the preparation of the manuscript.

Supplementary data

Supplementary data to this article can be found online at https://doi.org/10.1016/j.joca.2019.05.010.

References

1. Karczewski KJ, Snyder MP. Integrative omics for health and disease. Nat Rev Genet 2018;19:299.
2. Mobasheri A, Rayman MP, Gualillo O, Sellam J, van der Kraan P, Fearon U. The role of metabolism in the pathogenesis of osteoarthritis. Nat Rev Rheumatol 2017;13:302–11.
3. Thysen S, Luyten FP, Lories RJU. Targets, models and challenges in osteoarthritis research. Dis Model Mech 2015;8:17–30.
4. Spicer R, Salek RM, Moreno P, Cañueto D, Steinbeck C. Navigating freely-available software tools for metabolomics analysis. Metabolomics 2017;13:106.
5. Fiehn O. Metabolomics – the link between genotypes and phenotypes. Plant Mol Biol 2002;48:155–71.
6. Menni C, Zierer J, Valdes AM, Spector TD. Mixing omics: combining genetics and metabolomics to study rheumatic diseases. Nat Rev Rheumatol 2017;13:174.
7. Jaggard MKJ, Boulangé CL, Akhbari P, Vaghela U, Bhattacharya R, Williams HRT, *et al*. A systematic review of the small molecule studies of osteoarthritis using nuclear magnetic resonance and mass spectroscopy. Osteoarthritis Cartilage 2019;27:560–70.
8. Zhai G, Randell EW, Rahman P. Metabolomics of osteoarthritis: emerging novel markers and their potential clinical utility. Rheumatology 2018;57:2087–95.
9. Carlson AK, Rawle RA, Adams E, Greenwood MC, Bothner B, June RK. Application of global metabolomic profiling of synovial fluid for osteoarthritis biomarkers. Biochem Biophys Res Commun 2018;499:182–8.
10. Mickiewicz B, Kelly JJ, Ludwig TE, Weljie AM, Wiley JP, Schmidt TA, *et al*. Metabolic analysis of knee synovial fluid as a potential diagnostic approach for osteoarthritis. J Orthop Res 2015;33:1631–8.
11. de Sousa EB, de Farias GC, dos Santos Junior GC, Almeida FC, Duarte ML, Neto VM, *et al*. Normal and osteoarthritic synovial fluid present different metabolomic profile. Osteoarthritis Cartilage 2017;25:S384.
12. Adams Jr SB, Setton LA, Kensicki E, Bolognesi MP, Toth AP, Nettles DL. Global metabolic profiling of human osteoarthritic synovium. Osteoarthritis Cartilage 2012;20:64–7.
13. Zhai G, Wang-Sattler R, Hart DJ, Arden NK, Hakim AJ, Illig T, *et al*. Serum branched-chain amino acid to histidine ratio: a novel metabolomic biomarker of knee osteoarthritis. Ann Rheum Dis 2010;69:1227–31.
14. Li X, Yang S, Qiu Y, Zhao T, Chen T, Su M, *et al*. Urinary metabolomics as a potentially novel diagnostic and stratification tool for knee osteoarthritis. Metabolomics 2010;6:109–18.
15. Xu Z, Chen T, Luo J, Ding S, Gao S, Zhang J. Cartilaginous metabolomic study reveals potential mechanisms of osteophyte formation in osteoarthritis. J Proteome Res 2017;16:1425–35.

16. Shet K, Siddiqui SM, Yoshihara H, Kurhanewicz J, Ries M, Li X. High-resolution magic angle spinning NMR spectroscopy of human osteoarthritic cartilage. NMR Biomed 2012;25:538–44.
17. Borel M, Pastoureau P, Papon J, Madelmont JC, Moins N, Maublant J, *et al*. Longitudinal profiling of articular cartilage degradation in osteoarthritis by high-resolution magic angle spinning 1H NMR spectroscopy: experimental study in the meniscectomized Guinea pig model. J Proteome Res 2009;8:2594–600.
18. McCutchen CN, Zignego DL, June RK. Metabolic responses induced by compression of chondrocytes in variable-stiffness microenvironments. J Biomech 2017;64:49–58.
19. Chong KW, Chanalaris A, Burleigh A, Jin H, Watt FE, Saklatvala J, *et al*. Fibroblast growth factor 2 drives changes in gene expression following injury to murine cartilage *in vitro* and *in vivo*. Arthritis Rheum 2013;65:2346–55.
20. Stanton H, Golub SB, Rogerson FM, Last K, Little CB, Fosang AJ. Investigating ADAMTS-mediated aggrecanolysis in mouse cartilage. Nat Protoc 2011;6:388.
21. Dudzik D, Barbas-Bernardos C, Garcia A, Barbas C. Quality assurance procedures for mass spectrometry untargeted metabolomics. a review. J Pharm Biomed Anal 2018;147:149–73.
22. Alseekh S, Fernie AR. Metabolomics 20 years on: what have we learned and what hurdles remain? Plant J 2018;94:933–42.
23. Schauer N, Steinhauser D, Strelkov S, Schomburg D, Allison G, Moritz T, *et al*. GC–MS libraries for the rapid identification of metabolites in complex biological samples. FEBS (Fed Eur Biochem Soc) Lett 2005;579:1332–7.
24. Lisec J, Schauer N, Kopka J, Willmitzer L, Fernie AR. Gas chromatography mass spectrometry-based metabolite profiling in plants. Nat Protoc 2006;1:387–96.
25. Wickham H. ggplot2: Elegant Graphics for Data Analysis. New York: Springer-Verlag; 2016.
26. Team RC. R: A Language and Environment for Statistical Computing 2017.
27. Inc PT. Collaborative Data Science. Montréal, QC: Plotly Technologies Inc.; 2015.
28. Chong J, Soufan O, Li C, Caraus I, Li S, Bourque G, *et al*. MetaboAnalyst 4.0: towards more transparent and integrative metabolomics analysis. Nucleic Acids Res 2018;46(W1):W486–94, https://doi.org/10.1093/nar/gky310.
29. Kanehisa M, Goto S. KEGG: kyoto encyclopedia of genes and genomes. Nucleic Acids Res 2000;28:27–30.
30. Berenbaum F, Griffin TM, Liu-Bryan R. Review: metabolic regulation of inflammation in osteoarthritis. Arthritis Rheum 2017;69:9–21.
31. June RK, Liu-Bryan R, Long F, Griffin TM. Emerging role of metabolic signaling in synovial joint remodeling and osteoarthritis. J Orthop Res 2016;34:2048–58.
32. Bywaters EGL, MacKinnon M. The metabolism of joint tissues. J Pathol Bacteriol 1937;44:247–68.
33. Hoffmann A, Lehmann G, Wertheimer E. Der Glykogenbestand des Knorpels und seine Bedeutung. Pflugers Arch für Gesamte Physiol Menschen Tiere 1928;220:183–93.
34. Rosenthal O, Bowie MA, Wagoner G. Studies in the metabolism of articular cartilage. I. Respiration and glycolysis of cartilage in relation to its age. J Cell Comp Physiol 1941;17:221–33.
35. Gavriilidis C, Miwa S, von Zglinicki T, Taylor RW, Young DA. Mitochondrial dysfunction in osteoarthritis is associated with down-regulation of superoxide dismutase 2. Arthritis Rheum 2013;65:378–87.
36. Heywood HK, Bader DL, Lee DA. Rate of oxygen consumption by isolated articular chondrocytes is sensitive to medium glucose concentration. J Cell Physiol 2006;206:402–10.
37. Lane RS, Fu Y, Matsuzaki S, Kinter M, Humphries KM, Griffin TM. Mitochondrial respiration and redox coupling in articular chondrocytes. Arthritis Res Ther 2015;17:54.
38. Lee RB, Urban JP. Functional replacement of oxygen by other oxidants in articular cartilage. Arthritis Rheum 2002;46:3190–200.
39. Martin JA, Martini A, Molinari A, Morgan W, Ramalingam W, Buckwalter JA, *et al*. Mitochondrial electron transport and glycolysis are coupled in articular cartilage. Osteoarthritis Cartilage 2012;20:323–9.
40. Liu-Bryan R, Terkeltaub R. Emerging regulators of the inflammatory process in osteoarthritis. Nat Rev Rheumatol 2015;11:35–44.
41. Barker GA, Wilkins RJ, Golding S, Ellory JC. Neutral amino acid transport in bovine articular chondrocytes. J Physiol 1999;514:795–808.
42. Goberdhan Deborah CI, Wilson C, Harris Adrian L. Amino acid sensing by mTORC1: intracellular transporters mark the spot. Cell Metabol 2016;23:580–9.
43. Nicklin P, Bergman P, Zhang B, Triantafellow E, Wang H, Nyfeler B, *et al*. Bidirectional transport of amino acids regulates mTOR and autophagy. Cell 2009;136:521–34.
44. Sengupta S, Peterson TR, Sabatini DM. Regulation of the mTOR complex 1 pathway by nutrients, growth factors, and stress. Mol Cell 2010;40:310–22.
45. Cam H, Easton JB, High A, Houghton PJ. mTORC1 signaling under hypoxic conditions is controlled by ATM-dependent phosphorylation of HIF-1α. Mol Cell 2010;40:509–20.
46. Shapiro IM, Srinivas V. Metabolic consideration of epiphyseal growth: survival responses in a taxing environment. Bone 2007;40:561–7.
47. Carames B, Hasegawa A, Taniguchi N, Miyaki S, Blanco FJ, Lotz M. Autophagy activation by rapamycin reduces severity of experimental osteoarthritis. Ann Rheum Dis 2012;71:575–81.
48. Cole HA, Yuasa M, Hawley G, Cates JMM, Nyman JS, Schoenecker JG. Differential development of the distal and proximal femoral epiphysis and physis in mice. Bone 2013;52:337–46.
49. Stambough JL, Brighton CT, Iannotti JP, Storey BT. Characterization of growth plate mitochondria. J Orthop Res 1984;2:235–46.
50. Pollesello P, de Bernard B, Grandolfo M, Paoletti S, Vittur F, Kvam BJ. Energy state of chondrocytes assessed by 31P-NMR studies of preosseous cartilage. Biochem Biophys Res Commun 1991;180:216–22.
51. De Livera AM, Dias DA, De Souza D, Rupasinghe T, Pyke J, Tull D, *et al*. Normalizing and integrating metabolomics data. Anal Chem 2012;84:10768–76.
52. Gomes AP, Blenis J. A nexus for cellular homeostasis: the interplay between metabolic and signal transduction pathways. Curr Opin Biotechnol 2015;34:110–7.
53. Seifer DR, Furman BD, Guilak F, Olson SA, Brooks 3rd SC, Kraus VB. Novel synovial fluid recovery method allows for quantification of a marker of arthritis in mice. Osteoarthritis Cartilage 2008;16:1532–8.
54. Guma M, Tiziani S, Firestein GS. Metabolomics in rheumatic diseases: desperately seeking biomarkers. Nature reviews. Rheumatology 2016;12:269–81.